

University of Groningen

## Catchment response to lava damming: integrating field observation, geochronology and landscape evolution modelling

Van Gorp, Wouter; Schoorl, Jeroen M.; Temme, Arnaud J. A. M.; Reimann, Tony; Wijbrans, Jan R.; Maddy, Darrel; Demir, Tuncer; Veldkamp, Tom

*Published in:*  
Earth Surface Processes and Landforms

*DOI:*  
[10.1002/esp.3981](https://doi.org/10.1002/esp.3981)

**IMPORTANT NOTE: You are advised to consult the publisher's version (publisher's PDF) if you wish to cite from it. Please check the document version below.**

*Document Version*  
Publisher's PDF, also known as Version of record

*Publication date:*  
2016

[Link to publication in University of Groningen/UMCG research database](#)

### *Citation for published version (APA):*

Van Gorp, W., Schoorl, J. M., Temme, A. J. A. M., Reimann, T., Wijbrans, J. R., Maddy, D., Demir, T., & Veldkamp, T. (2016). Catchment response to lava damming: integrating field observation, geochronology and landscape evolution modelling. *Earth Surface Processes and Landforms*, 41(11), 1629-1644. <https://doi.org/10.1002/esp.3981>

### **Copyright**

Other than for strictly personal use, it is not permitted to download or to forward/distribute the text or part of it without the consent of the author(s) and/or copyright holder(s), unless the work is under an open content license (like Creative Commons).

The publication may also be distributed here under the terms of Article 25fa of the Dutch Copyright Act, indicated by the "Taverne" license. More information can be found on the University of Groningen website: <https://www.rug.nl/library/open-access/self-archiving-pure/taverne-amendment>.

### **Take-down policy**

If you believe that this document breaches copyright please contact us providing details, and we will remove access to the work immediately and investigate your claim.

Downloaded from the University of Groningen/UMCG research database (Pure): <http://www.rug.nl/research/portal>. For technical reasons the number of authors shown on this cover page is limited to 10 maximum.

# Catchment response to lava damming: integrating field observation, geochronology and landscape evolution modelling

Wouter van Gorp,<sup>1,2\*</sup> Jeroen M. Schoorl,<sup>1</sup> Arnaud J. A. M. Temme,<sup>1</sup> Tony Reimann,<sup>1</sup> Jan R. Wijbrans,<sup>3</sup> Darrel Maddy,<sup>4</sup> Tuncer Demir<sup>5</sup> and Tom Veldkamp<sup>6</sup>

<sup>1</sup> Soil Geography and Landscape Group, Wageningen University, Wageningen, The Netherlands

<sup>2</sup> Groningen Institute of Archaeology (GIA), University of Groningen, Groningen, The Netherlands

<sup>3</sup> Department of Earth Science, Vrije Universiteit, Amsterdam, The Netherlands

<sup>4</sup> School of Geography, Politics and Sociology, University of Newcastle, Newcastle-upon-Tyne, UK

<sup>5</sup> Department of Geography, Faculty of Letters, Akdeniz University, Antalya, Turkey

<sup>6</sup> Faculty Geo-Information Science and Earth Observation (ITC), University of Twente, Enschede, The Netherlands

Received 11 June 2015; Revised 22 May 2016; Accepted 23 May 2016

\*Correspondence to: Wouter van Gorp, Groningen Institute of Archaeology (GIA), University of Groningen, Poststraat 6, 9712 ER, Groningen, The Netherlands. E-mail: w.van.gorp@rug.nl

ESPL

Earth Surface Processes and Landforms

**ABSTRACT:** Combining field reconstruction and landscape evolution modelling can be useful to investigate the relative role of different drivers on catchment response. The Geren Catchment (~45 km<sup>2</sup>) in western Turkey is suitable for such a study, as it has been influenced by uplift, climate change and lava damming. Four Middle Pleistocene lava flows (<sup>40</sup>Ar/<sup>39</sup>Ar- dated from 310 to 175 ka) filled and dammed the Gediz River at the Gediz–Geren confluence, resulting in base-level fluctuations of the otherwise uplift-driven incising river. Field reconstruction and luminescence dating suggest fluvial terraces in the Geren Catchment are capped by Middle Pleistocene aggradational fills. This showed that incision of the Geren trunk stream has been delayed until the end of MIS 5. Subsequently, the catchment has responded to base-level lowering since MIS 4 by 30 m of stepped net incision. Field reconstruction left us with uncertainty on the main drivers of terrace formation. Therefore, we used landscape evolution modelling to investigate catchment response to three scenarios of base-level change: (i) uplift with climate change (rainfall and vegetation based on arboreal pollen); (ii) uplift, climate change and short-lived damming events; (iii) uplift, climate and long-lived damming events. Outputs were evaluated for erosion–aggradation evolution in trunk streams at two different distances from the catchment outlet. Climate influences erosion–aggradation activity in the catchment, although internal feedbacks influence timing and magnitude. Furthermore, lava damming events partly control if and where these climate-driven aggradations occur. Damming thus leaves a legacy on current landscape evolution. Catchment response to long-duration damming events corresponds best with field reconstruction and dating. The combination of climate and base level explains a significant part of the landscape evolution history of the Geren Catchment. By combining model results with fieldwork, additional conclusions on landscape evolution could be drawn. Copyright © 2016 John Wiley & Sons, Ltd.

**KEYWORDS:** lava damming; catchment response; field–LEM combination; landscape evolution modelling; argon/argon dating; luminescence dating

## Introduction

The impact of natural damming on catchment evolution can be significant, especially on 10<sup>3</sup>–10<sup>4</sup> year timescales (Korup *et al.*, 2006; Maddy *et al.*, 2012a; Van Gorp *et al.*, 2013; Van Gorp *et al.*, 2014; Van Gorp *et al.*, 2015). Common causes for natural dams are landslides, debris flows, glaciers, glacial moraines, lahars, pyroclastic flows and lava flows (Korup and Tweed, 2007; O'Connor *et al.*, 2013). Their longevity depends for a large part on dam size, shape and composition (e.g. Capra, 2007). For instance landslide dams are usually short-lived (Ermini and Casagli, 2003). Lava dams are not as widespread as for instance landslide dams. However, their impact on catchment evolution can be significant due to their relatively high

longevity and because they can fill river valleys over several kilometres (O'Connor and Beebe, 2009). This promotes their preservation and therefore also preservation of palaeo-valleys. Lava dams furthermore provide a direct age constraint of the damming event. Recent studies from Kenya (Veldkamp *et al.*, 2012), the United States (Crow *et al.*, 2008; Ely *et al.*, 2012), Australia (Roach *et al.*, 2008) and Turkey (Maddy *et al.*, 2012a; Van Gorp *et al.*, 2013) indicate the significance of lava dams for fluvial evolution on Quaternary timescales. Field reconstruction and dating of both lavas and fluvial deposits often reveal direct impacts such as stream rerouting, lake formation, infilling and dam removal. However the long-term response of upstream catchment evolution is hard to illustrate from fieldwork alone. In this case, a landscape evolution model

(LEM) can be a useful tool to investigate the relative role of different drivers on catchment response, using field information on timing of damming events as an input and known catchment history, such as dated terraces, for evaluation. The Geren Catchment, a small (45 km<sup>2</sup>) upland watershed in western Turkey, is suitable for such a study, because its base level has been influenced by volcanic damming in the Holocene (Van Gorp *et al.*, 2013). The presence of older valley-filling lava flow remnants near the Geren outlet (Westaway *et al.*, 2004) suggests that the Geren has been influenced by damming during the Middle and Late Pleistocene as well.

Upland catchment response to lava damming has been modelled using an artificial catchment, demonstrating knickpoint persistence, delayed incision, sediment storage and stream reroutings on top of lake deposits (Van Gorp *et al.*, 2014). Subsequent model work on catchment response to damming calibrated for the Geren Catchment already revealed how it responds at a 300 ka scale to lava dams under an uplifting regime (Van Gorp *et al.*, 2015). Modelling results showed dampened incision and denudation of streams and slopes, an effect that migrates upstream. This dampening can subsequently be overtaken by renewed incision pulses through streams, leading to decoupled landscape response. These results are valuable because they demonstrate that long-term response to damming can be observed and modelled in a catchment such as the Geren. However, in that study, the goal was more conceptual and rainfall was held constant, while damming events were short (1 ka) and occurred once each 100 ka. Thus, some field-site specific information such as timing and duration of observed lava dams as well as climate data was not used.

The combination of field-derived landscape reconstruction with landscape evolution modelling is a promising methodology to understand landscape evolution, not only of specific field areas but also by disclosing feedbacks or responses that can have a wider impact (Temme and Veldkamp, 2009). Fieldwork will always be indispensable because stratigraphic and landscape context cannot be derived without field observations, field sampling for dating or other types of analyses. Nevertheless, many landscape reconstruction studies are done by conducting fieldwork alone, while modelling studies are often only conceptual.

## Aim

The aim of this paper is to demonstrate how field-based reconstruction and landscape evolution modelling can complement each other in understanding catchment response to base level change. The case study area used in this paper is the Geren catchment, chosen because it has been influenced by damming events (Van Gorp *et al.*, 2013; Van Gorp *et al.*, 2015). Specific objectives for the Geren Catchment are two-fold: (i) to reconstruct the 300 ka lava damming history of the Geren Catchment and Geren Catchment evolution using field-derived information and chronological data; (ii) to use a LEM to clarify uncertainties which emerge from this field reconstruction and to test the relative importance of base-level change and rainfall on catchment evolution. Finally, model results are evaluated with independent field to obtain new insights into the drivers of Geren Catchment evolution.

## Regional setting

The Geren Catchment is a small tributary of the Upper Gediz River and is located in the Kula volcanic area, western Turkey. Here, the Gediz River is currently draining into the

east–west oriented Aleşehir graben. The Gediz is traversing Miocene interior basin fills (Maddy *et al.*, 2007) which are enclosed and underlain by metamorphic and metasedimentary basement rocks (e.g. Purvis and Robertson, 2004). These basin fills consist of a fining upward sequence (e.g. Seyitoglu, 1997), with deformed conglomerates and sands of the Hacibekir group at the base, which are unconformably overlain by fluviolacustrine deposits of the Inay group. The lower part of the Inay group consists of fluvial gravels and sands, fining up to silts forming the Ahmetler formation. This formation is overlain by lake-accumulated tephtras which originated from Miocene stratovolcanoes, and which are topped by lacustrine limestones of the Ulubey formation. The onset of formation of the Aleşehir graben influenced local drainage patterns which, together with erosion driven uplift, caused basin inversion (Westaway *et al.*, 2004; Maddy *et al.*, 2007; Maddy *et al.*, 2012b) and the Ulubey limestones now form plateaux in the study reach. Subsequent fluvial incision of the basin fills by the Gediz has mainly been driven by regional uplift and climate variability in the Early Pleistocene (Maddy *et al.*, 2012b). However, the Kula volcanic area is increasingly recognized as an area where lava damming has influenced fluvial evolution of the Gediz River and its tributaries since the onset of volcanism in the early Pleistocene until the present (Maddy *et al.*, 2007; Maddy *et al.*, 2012a; Van Gorp *et al.*, 2013; Maddy *et al.*, 2015). Three volcanism groups have been categorized: early Pleistocene  $\beta_2$ , Middle Pleistocene  $\beta_3$ , and most recent  $\beta_4$  lavas (Richardson-Bunbury, 1996). Early Pleistocene landscape reconstruction has benefited from clear preservation of Gediz terraces capped by  $\beta_2$  lavas (Maddy *et al.*, 2012a; Maddy *et al.*, 2012b; Maddy *et al.*, 2015). However, evolution of the Gediz in the period between 1 Ma and the Middle Pleistocene remains poorly understood due to lack of documented preserved records along both the Gediz and its tributaries such as the Geren. Fluvial terrace remnants from the period after volcanic activity restarted ( $\beta_3$  group) are better represented. Radiometric lava ages between 250 to 100 ka have been reported (Richardson-Bunbury, 1996; Westaway *et al.*, 2004; Westaway *et al.*, 2006). Most of these dates cluster between 100 and 200 ka. Some of these dated lavas overlie Gediz River terraces (Westaway *et al.*, 2004), such as below the Söğüt flow unit upstream of the Geren outlet and the Palankaya flow downstream of the Geren Catchment outlet (Figure 1) which have been <sup>40</sup>K/<sup>40</sup>Ar dated to 236 ± 6 ka and 175 ± 3 ka, respectively (Westaway *et al.*, 2006). However, near the Gediz–Geren confluence, there is no relation between dated lavas and fluvial terraces and thus a clear link between lava flows and Middle Pleistocene fluvial landscape evolution could not be made. The youngest lavas are of Holocene age and are sometimes located adjacent to current river level, such as near the Gediz–Geren confluence, where the 3–2.6 ka dated Kula flow (Figure 1) dammed the Gediz and Geren Rivers (Van Gorp *et al.*, 2013).

## Materials and Methods

### Approach

In this paper landscape evolution modelling and fieldwork are combined. First, fieldwork and dating results are presented. Second, the sequence of Middle Pleistocene to Holocene lava damming events which influenced the Geren Catchment outlet is reconstructed. This reconstruction of damming events is then translated into three model scenarios for an input base-level curve for a 300 ka LEM simulation. Finally, modelling results

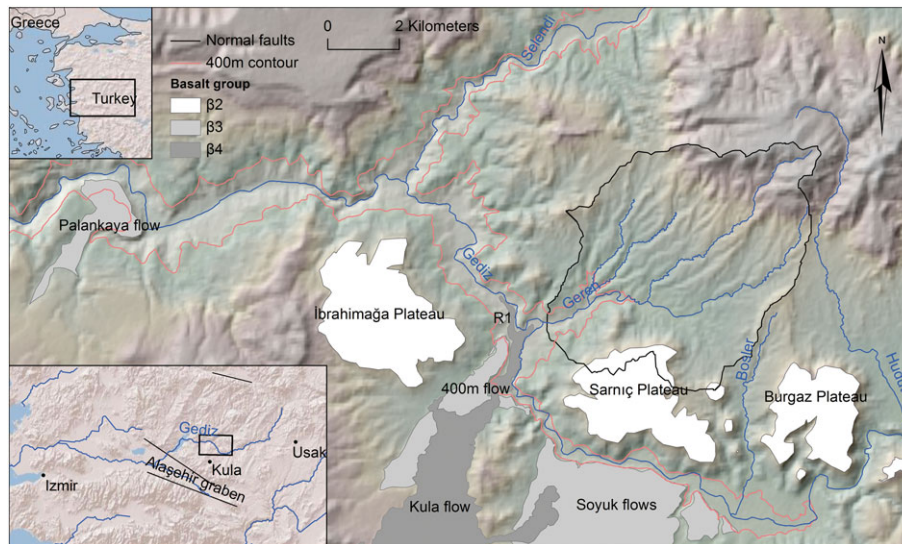


**Figure 1.** Location and overview of the upper Gediz–Geren area with some of the main volcanic units. Black line depicts Gerem Catchment limits. This figure is available in colour online at [wileyonlinelibrary.com/journal/espl](http://wileyonlinelibrary.com/journal/espl)

of Gerem Catchment evolution are presented and discussed together with the fieldwork results.

## Fieldwork

During fieldwork campaigns in 2009–2012, geomorphology of the Gerem Catchment and the Gerem–Gediz confluence area was mapped. Palaeosurfaces and fluvial terraces were recorded as well as areas with limestone-derived fluvial gravels and fine-grained sediments. Individual lava flows and their relation with palaeo-Gediz valleys were determined. Samples for dating of lavas and sediments were taken.

## Elevation model

Using ALOS-PRISM stereo-satellite imagery, a digital elevation model (DEM) was reconstructed with the DEM-extraction tool of ENVI 4.7. Ground control points were taken using a Sokkia dGPS. The extracted 3 m resolution DEM was resampled to 30 m for modelling purposes. A palaeo-DEM was created from a reconstruction and interpolation of palaeosurfaces. It represents the 300 ka landscape and is the same as used in Van Gorp *et al.* (2015). It was derived by interpolating palaeosurfaces and creating a hydrologically correct DEM with an outlet at 390 m, which is based on the Gediz terrace capping the post-310.5 ka lava flow of Ar-4. No drainage network was artificially incised into this DEM. The overall drainage pattern of the current Gerem Catchment emerges from the reconstructed palaeo-DEM, with three main northern branches draining into the southern trunk (see Figure 2, Van Gorp *et al.*, 2015).

## Radiocarbon dating

Radiocarbon dating was carried out on an organic rich sample from fine layered mud-deposits using accelerator mass spectrometry (AMS) at the Centre for Isotope Research, University of Groningen, the Netherlands (Gott dang *et al.*, 1995). Conversion of carbon-14 years before present ( $^{14}\text{C}$  yr. BP) to calibrated years before present (cal yr. BP) was undertaken using the IntCal04 calibration curve (Reimer *et al.*, 2004) and the WinCal25 calibration program (see Supporting Information Appendix S1).

## $^{40}\text{Ar}/^{39}\text{Ar}$ dating

Basaltic samples were taken for  $^{40}\text{Ar}/^{39}\text{Ar}$  radio-isotopic dating from locations with a stratigraphical relation to the fluvial valley they filled. Age estimates were obtained by incremental heating experiments carried out at the Vrije Universiteit, Amsterdam, the Netherlands. Groundmass separates were prepared by obtaining homogenous fragments of microcrystalline groundmass to minimize the chance of inherited argon (Ar) from phenocryst phases (Wijbrans *et al.*, 2011). Data reduction and age calculations were made using ArArCalc v2.5 (Koppers, 2002). The detailed procedure is described in Van Gorp *et al.* (2013), Schoorl *et al.* (2014a) and Maddy *et al.* (2015). Detailed age data are presented in the Supporting Information Appendix S2.

## Luminescence dating

Luminescence dating was carried out on fluvial sands of six samples. In this method the burial time of sand or silt deposits is estimated. The amount of ionizing radiation received by quartz or feldspar grains (palaeodose, Gy) since the time of burial is determined by measuring a light signal emitted by the minerals. The annual ionizing radiation dose received from surrounding materials is also determined (dose rate, Gy/ka). Luminescence age is then determined by:

$$\text{Age(ka)} = \text{palaeodose(Gy)} / \text{dose rate(Gy/ka)} \quad (1)$$

Measurements were carried out at the Netherlands Centre for Luminescence Dating, Delft University of Technology and Wageningen University, the Netherlands. Earlier experience with fluvial sediments from the study area showed that luminescence sensitivity of the quartz fraction is too low (Van Gorp *et al.*, 2013) for accurate optically stimulated luminescence (OSL) dating. Therefore, the sand-sized (180–212  $\mu\text{m}$ ) K-rich feldspar fraction was used for infra-red stimulated luminescence (IRSL) dating although the feldspar luminescence signals may be affected by anomalous fading, which potentially causes age underestimation (Wallinga *et al.*, 2007). To avoid or reduce this effect the post-IR IRSL signal was used (Thomsen *et al.*, 2008, Buylaert *et al.*, 2012, Kars *et al.*, 2012). For four samples we used conventional multiple-grain

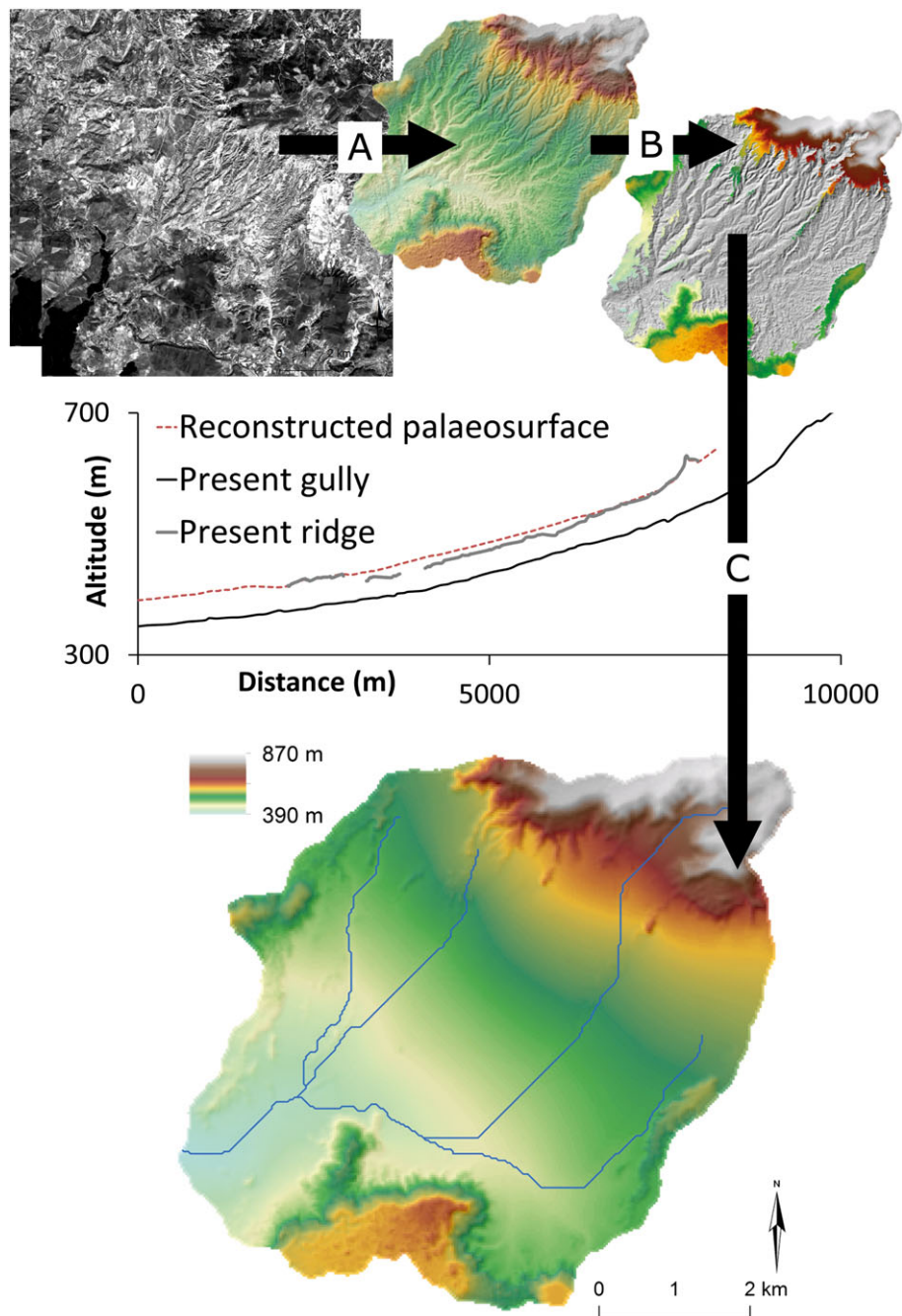


**Figure 2.** (A) DEM-extraction from a forward and backward image pair of ALOS-PRISM panchromatic satellite imagery. (B) Extraction of ridges 40 m above current river level. (C) Interpolation of a palaeo-DEM area, using a 390 m elevation outlet area (after Van Gorp *et al.*, 2015). This figure is available in colour online at [wileyonlinelibrary.com/journal/espl](http://wileyonlinelibrary.com/journal/espl)

subsamples where a bulk pIRIR feldspar signal from 50 to 100 grains is measured. To reduce the unwanted effects of thermal transfer and residual dose, which are especially important for young Holocene samples (Reimann *et al.*, 2011), we made use of a low-temperature pIRIR signal (Reimann and Tsukamoto, 2012) for the three samples which turned out to be Holocene and applied the pIRIR K-feldspar single-grain procedure described in Reimann *et al.* (2012) to these three samples. For details on measurement procedures, the reader is referred to the Supporting Information Appendix S3.

## Model

LEM LAPSUS (Schoorl *et al.*, 2000; Schoorl *et al.*, 2002; Temme and Veldkamp, 2009) was used to simulate a 300 000 yr. period of landscape evolution of the Geren Catchment. In the

remainder of the text, the notation 'ka' is used for field reconstructed ages in ka, while 'yr' is used for simulation runtime, where yr. 0 is equivalent to 300 ka ago and 300 000 yr. to present. LAPSUS is a grid-based model which models water runoff erosion and deposition. It routes water and sediment using a multiple flow approach, which allows water to flow downslope over multiple cells instead of only the cell with steepest descent (Freeman, 1991; Quinn *et al.*, 1991) and calculates sediment transport capacity  $C$  over time  $t$  (yr) and space  $s$  (in metres) between a cell and each of its downslope neighbours following Kirkby (1971).

$$C_{s,t} = Q_{s,t}^m \cdot \Lambda_{s,t}^n \quad (2)$$

where  $Q_{s,t}$  is fractional discharge (in metres) and  $\Lambda$  tangent of slope (–). Parameter  $m$  is the discharge, and  $n$  the slope

exponent (Kirkby, 1971). The amount of sediment  $S$  (in metres) that will be transported over one cellsize length depends on transport capacity  $C$  and sediment already in transport  $S_0$  (in metres) and is calculated according to Foster and Meyer (1972, 1975):

$$S_{s,t} = C_{s,t} + (S_{0s,t} - C_{s,t}) \cdot e^{-\text{cellsize}/h} \quad (3)$$

where  $h$  is an erodibility or sedimentation factor. When sediment already in transport is smaller than transport capacity, erosion occurs and  $h$  is calculated as follows:

$$h_{s,t} = \frac{C_{s,t}}{K_{s,t} \cdot Q_{s,t} \cdot A_{s,t}} \quad (4)$$

where  $K$  (in  $\text{m}^{-1}$ ) is an erodibility factor. If the amount of sediment already in transport is larger than transport capacity  $C$ , deposition will occur and  $h$  is calculated as follows:

$$h_{s,t} = \frac{C_{s,t}}{P_{s,t} \cdot Q_{s,t} \cdot A_{s,t}} \quad (5)$$

where  $P$  (in  $\text{m}^{-1}$ ) is a sedimentation factor. Thus,  $K$  and  $P$  represent lumped surface characteristics of a gridcell and have been used as calibration factors (Schoorl *et al.*, 2000; Schoorl *et al.*, 2002; Schoorl *et al.*, 2004; Temme and Veldkamp, 2009; Baartman *et al.*, 2012; Van Gorp *et al.*, 2015). Furthermore, LAPSUS can deal with non-spurious sinks dynamically (Temme *et al.*, 2006). For recent further explanations of model behaviour, the reader is referred to Van Gorp *et al.* (2015) and Schoorl *et al.* (2014b).

The model scenario setup will be discussed later, because its explanation requires fieldwork results, which will be presented in the next section ('Fieldwork and dating results').

## Fieldwork and Dating Results

We will present field results according to three areas: (A) the Gediz–Geren confluence; (B) the downstream Geren area; (C) the upstream tributary streams (see Figure 3).

### The Geren–Gediz confluence

Several indications for base-level change have been found in the Gediz–Geren confluence area. Those associated with the Holocene 'Kula flow' have been discussed by Van Gorp *et al.* (2013). Here, we present and discuss field evidence for earlier lava dams. Remnants of  $\beta 3$  lava flows are located 1 km downstream of the Geren confluence, at the left bank of the Gediz River (Richardson-Bunbury, 1996). Here, a lava tongue which filled the former Gediz valley originates from the south. These lavas consist of at least two different stacked flows (Ar-3bottom and Ar-3top, Figure 3), separated by a sandy layer containing fluviially transported tephra. Just downstream, an isolated lava remnant (Ar-4, Figure 3, see also Figure 4C) with unclear relationship to either flow is found. This remnant is both underlain and overlain by fluvial gravels, evidencing a phase of base-level rise of the Gediz since the establishment of this lava flow before the river incised to its current level.

The Gediz River has an estimated long-term incision rate of  $0.14 \text{ mm a}^{-1}$  (Maddy *et al.*, 2012b) over a Ma extent. Early Pleistocene dams caused mild disturbance to this incision rate, whereas tributary streams were affected more severely in the form of channel infilling and stream diversions (Maddy *et al.*, 2012a). The Middle Pleistocene damming situation near the Geren–Gediz confluence differs from those in the Early Pleistocene in the sense that the Gediz valley was more confined than in the Early Pleistocene and, therefore, lava flows have repeatedly entered the same valley. At least two of the newly dated Middle Pleistocene lava flows have filled the Gediz valley and dammed the Geren Catchment. The lava flow at IR-4 is

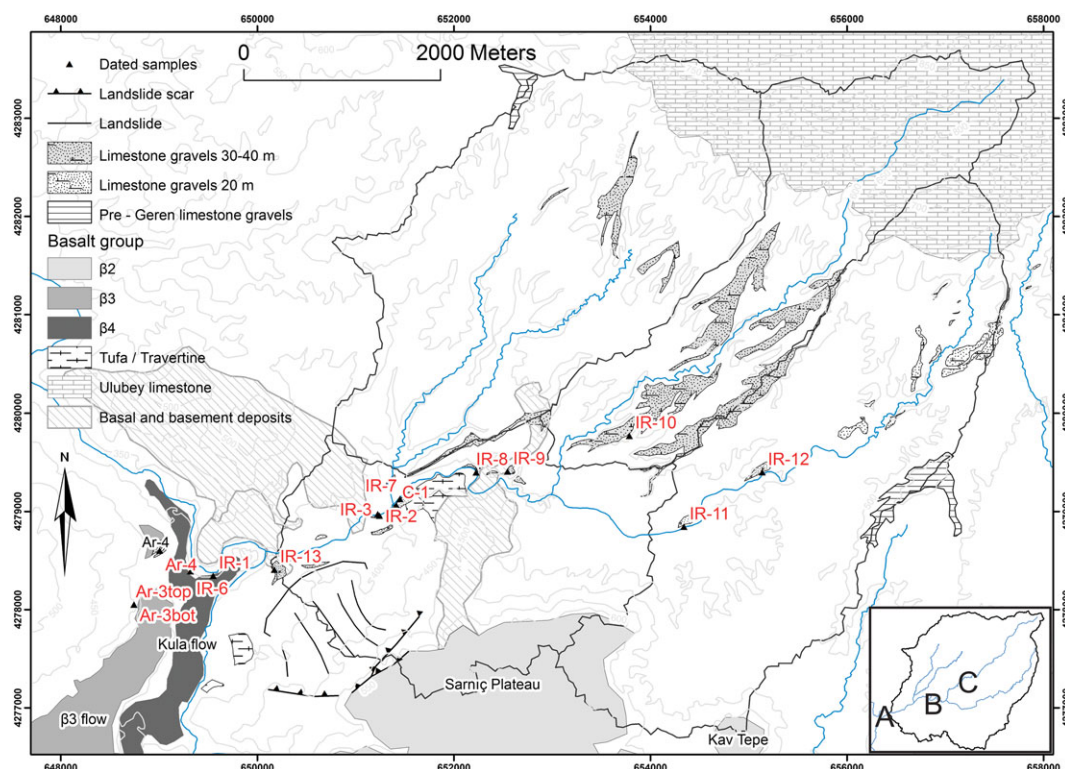


**Figure 3.** Study area, showing (i) main geological and geomorphological units, approximate elevation of limestone deposits above current stream level is indicated in legend, (ii) locations and names of dated samples. Inset shows key areas A–C (see main text). This figure is available in colour online at [wileyonlinelibrary.com/journal/espl](http://wileyonlinelibrary.com/journal/espl)  
Copyright © 2016 John Wiley & Sons, Ltd.

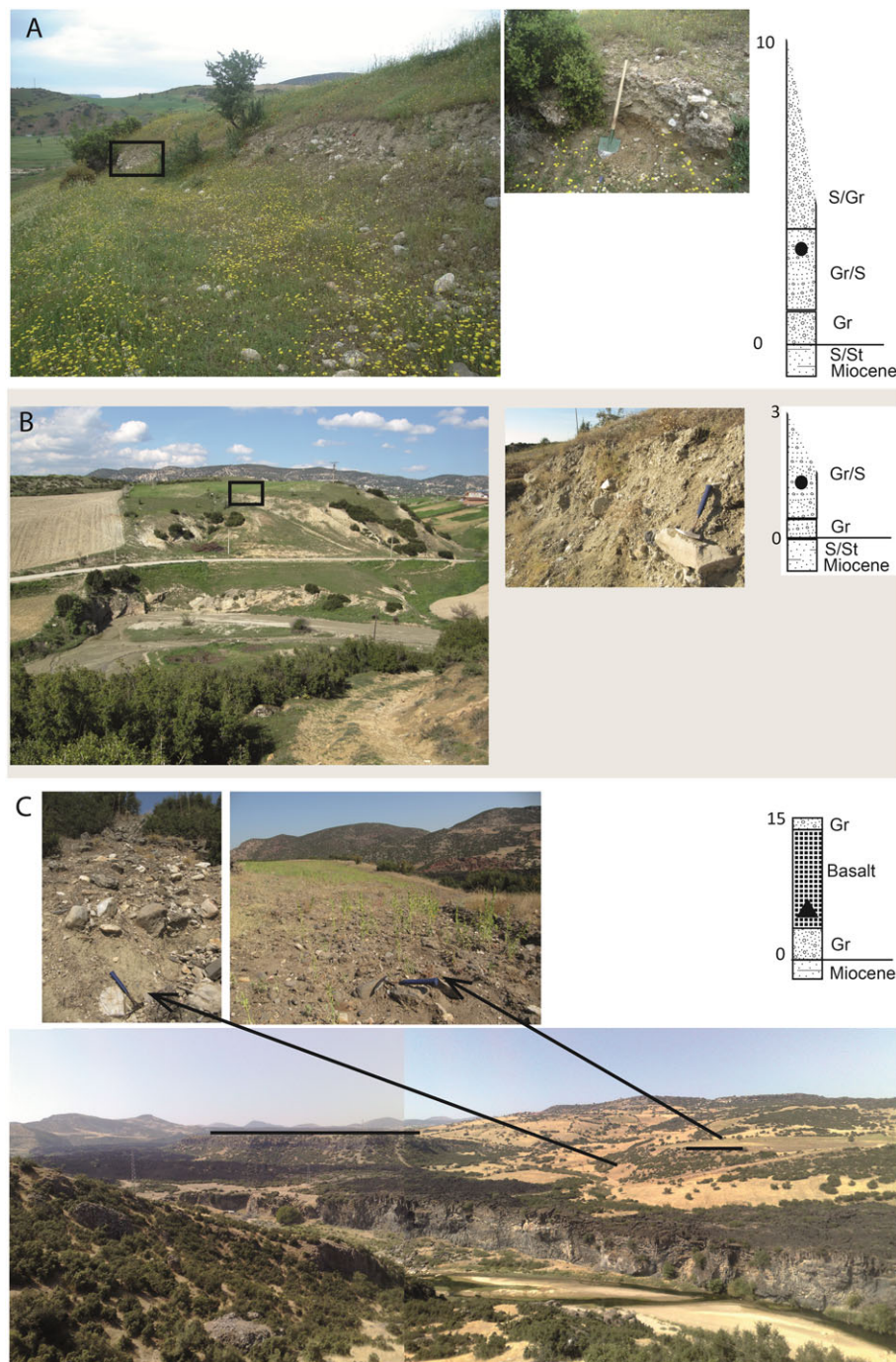


**Figure 4.** (A) Gediz terrace IR-13. (B) Location of Gerem terrace IR-9. (C) Location of Gediz terrace below and on top of lava dam Ar-4. Tops of lava flows are indicated by horizontal lines. Note that sediment logs are not scaled to the photographs. Sample locations are indicated in the sediment logs. Circles indicate luminescence dated samples, triangles indicate radiocarbon dated samples. This figure is available in colour online at [wileyonlinelibrary.com/journal/espl](http://wileyonlinelibrary.com/journal/espl)

both underlain and overlain by a fluvial terrace. Its age estimate of 311 ka thus provides a minimum age for the location of the pre-lava river valley at an elevation around 372 m, approximately 25 m above present river level. The river terrace on top of lava Ar-4 is located at  $\pm 390$  m elevation. The river level thus has risen by  $\pm 20$  m since establishment of flow Ar-4. The top of the 'β3 flow', at sample location Ar-3top, is around 400–410 m elevation. This upper lava flow is about 20 m thick. Rubbly material containing scoria and tephra has been observed at the end of the flow. This may be due to interaction of the lava with water, which is known to create ashes and scoria. This interaction probably took place, as the 'β3 flow' likely flowed over the contemporary Gediz valley-floor or perhaps entered the lake formed by lava flow Ar-4.

About 200 m southeast of the Gediz–Gerem confluence, a calcium carbonate ( $\text{CaCO}_3$ )-cemented fluvial terrace is present on top of Hacibekir conglomerates at around 375 m above sea level (a.s.l.), approximately 20–25 m above present river level (IR-13, Figures 3 and 4A). It can be traced along the slope and its planform resembles a meander loop. This terrace is buried by a gravel-bearing sandy aggradational fill of up to 10 m thick, reaching up to 385 m a.s.l., 30–35 m above current river level. This fill shows fluvial sand layers and gravel bands which contain rounded basalts and limestones. Its original thickness is unknown, as the top is not preserved. This whole sediment body resembles a fluvial terrace buried by a deltaic infill. Fluvial sand from the base of the infill has been sampled for luminescence dating (IR-13). Upslope of this aggradation, a large

landslide is present, containing large (up to 200 m<sup>3</sup>) basalt blocks from the edge of the Sarniç Plateau (Figure 3). It has an observed base around 40 m above current river level. A direct contact has not been observed but field relations suggest that this landslide entered the valley of the palaeo-Gediz around the time of IR-13. Further south, a partly collapsed travertine mound is present (Van Gorp *et al.*, 2013), with a current top around 400 m a.s.l.

### The downstream Geren area

Along the trunk stream of the lower Geren, several fluvial terraces and aggradational fills are observed at different elevations above current river level. The lowest fills usually have their base around 0.5 to 1 m above current river level. Aggradational fills at similar heights above current river level are observed at different locations upstream. Some have already been described by Van Gorp *et al.* (2013) and turned out to be Holocene (IR-3 and IR-4). At location IR-8, an 8 m thick sandy fining-upwards sequence is present, with its base around 0.5 to 1 m above current river level. The bottom part contains gravel bands, which diminish towards the top. A fine sandy layer around 2.5 m above current river level was sampled for dating. Location IR-11 contains 4 m of fluvial sands and gravels, with its base around 1 m above current river level. These gravels contain basalts, limestone and pottery at several locations. A sandy layer has been sampled for luminescence dating (IR-11). At locations C-1 and IR-7 (Figures 3 and 5), a fluvial aggradational fill consisting of several sedimentary units is observed. The base of around 4 m thick fluvial deposits is observed around 5 m above current river level and consists of mainly gravels in a silty matrix, alternating with gravel bands. This fluvial body is overlain by a sedimentary body which is associated with tufa formation and which is tentatively classified as paludal (cf. Pedley *et al.*, 2003). At its downstream side the fluvial unit is overlain by fine layered muddy lime deposits, sometimes intercalated with dark coloured muds, probably due to enrichment of organic material. Other layers contain calcified organic macro-remains, mainly reed stems and seeds, and some layers are almost entirely calcified into tufa layers with a phytoherm structure. Such a layer at the base of the muddy deposit was sampled for radiocarbon dating (C-1). Upstream of C-1, the fluvial deposits are overlain by light-coloured limestone-rich fine sands, which are capped by tufas up to around 20 m above current river level. The sands were sampled for luminescence dating (IR-7) about 1 m below the top of the sequence. From the exposure it is unclear how these muds and sands are related. The genesis of this sediment body is reconstructed as follows: the base consists of sediments of a

braided Geren River, which becomes abandoned. The upper part is unique for the area and has a more local character, influenced by nearby springs and tufa formation [e.g. analogous to Kaufmann *et al.* (2002)]. This deposit may be the infill of an abandoned Geren channel which has been cut off and choked with sediments, finally becoming a shallow water environment with fluctuating water table. The sediments of IR-7 are topped by a tufa and afterwards, or perhaps already partly during tufa formation, a channel incision of 20 m has taken place. Just upstream of this tufa, another, more extensive tufa body is present (Figure 3). Its base is not visibly overlying fluvial deposits, but its landscape position and lobate nature suggest that it is a perched springline deposit which entered a palaeo-Geren valley. Its top is around 400 m. The tufas, sands and muds of IR-7 and C-1 appear to be inset into and thus younger than this tufa body.

Location IR-9 is a 3 m thick fluvial terrace consisting of gravel and sand bars. It contains imbricated gravels consisting of subrounded basalts and limestones as well as subangular limestones. Its base is located around 30 m above current river level (Figure 4B). A sample for luminescence dating has been taken from a sandy layer.

### The upstream Geren streams

Upstream of IR-9, a main tributary draining the central part of the limestone plateau joins the trunk stream (Figure 3). Comparison of this stream to the trunk stream shows them to be quite different. The upper part of this tributary, which extends into the northern limestone plateau, has a gradient which is comparable to other tributaries further west. This stream is located in a narrow gorge bordered by limestone-capped ridges which are on average 30–40 m higher than the current stream and extend from the Ulubey limestone scar in the north to the confluence with the Geren trunk stream. Limestone ridges are now present as either elongated or fork-shaped ridges in the landscape. Similar fork-like ridges are observed at locations without limestone deposits. Location IR-10 is a fine layered sandy-silty sediment body of at least 15 m thickness, which is part of one of the elongated ridges. Its distal base contains fluvial gravels and coarse sands with crossbedding which are sometimes cemented. Sample IR-10 was taken around 35–40 m above current river level, which suggests correlation, by simple gradient extrapolation, with sample IR-9 and IR-13 (Figure 6). The eastern trunk stream has a less steep gradient and is bordered by ridges which are around 20 m higher than current stream level and which are sometimes limestone-capped. Location IR-12 consists of fluvial sands and gravels, entirely consisting of limestone clasts. Their base was difficult to observe but a sample for luminescence

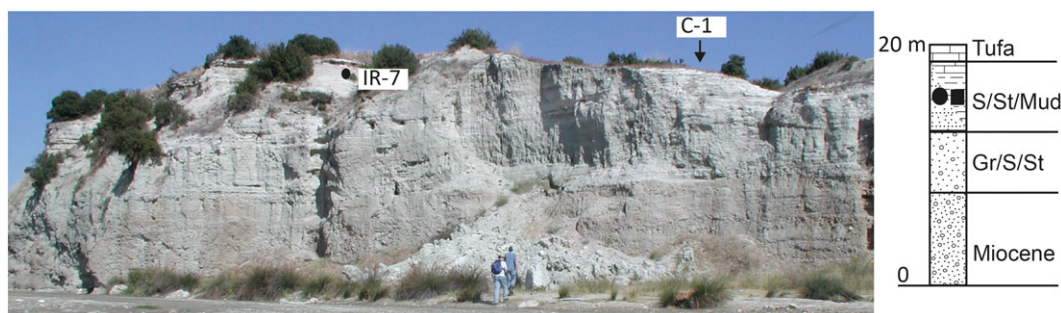


**Figure 5.** Overview and sediment log including sample setting of IR-7 and C-1. Person in blue is 1.90 m. Sample locations are depicted in the sediment log. Circles indicate luminescence dated samples, square indicates radiocarbon dated sample. This figure is available in colour online at [wileyonlinelibrary.com/journal/esp](http://wileyonlinelibrary.com/journal/esp)



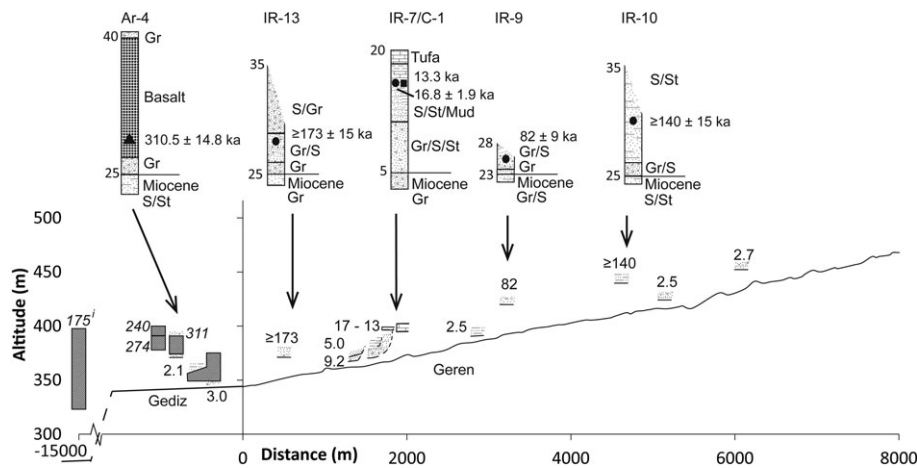


**Figure 6.** Sample elevations and dates plotted along the trunk stream of the Gerén Catchment. For selected samples, sediment logs are displayed. Triangles indicate dated lava, circles indicate luminescence dated samples, squares indicate radiocarbon dated samples (calibrated age displayed).

dating was taken from a sandy layer around 10 m above current river level.

### $^{40}\text{Ar}/^{39}\text{Ar}$ dating results

Westaway *et al.* (2006) presented an age of  $180 \pm 5$  ka from a flow near the Gediz valley and linked this age to the flow remnant at location Ar-4 (Figure 3) which overlies a fluvial terrace. However, their sample location is at least 5 km south and upslope of Ar-4. There are different possible cones that could have produced flows, some of them reaching the Gediz River. Steps in the surface of the lava flows have been interpreted to be flow fronts [e.g. Figure 4 in Westaway *et al.* (2004)], but there are also topographical indications that the lava flowed over terrace bluffs. Either way, making a link from the  $180 \pm 5$  ka date to the Ar-4 lava is difficult. Only the Palankaya flow, 15 km downstream of the Gediz–Gerén confluence, is dated in stratigraphical correlation with the Gediz River (Westaway *et al.*, 2006). Therefore, in the present study, three  $\beta_3$  lavas near the Gediz–Gerén outlet were sampled for dating. Sample location Ar-4 has a lowest observed base around 372 m and is on top of and overlain by a fluvial terrace at 390 m (Figure 4C). The two stacked lava flows at Ar-3bottom and Ar-3top are at the tip of the lava tongue which entered the Gediz valley from the south.

Sample Ar-4 is dated to  $311 \pm 15$  ka, sample Ar-3a is dated  $274 \pm 13$  ka and sample Ar-3b is dated  $240 \pm 18$  ka, (Table I). This last sample interestingly coincides with an age of  $236 \pm 6$  ka (Westaway *et al.*, 2006) of a  $\beta_3$  lava near the north-eastern edge of the Söğüt flows (Figure 1) and could, in theory, represent the same eruption. These new dates suggest that at least three different flows entered the Gediz River within a time span of 70 ka.

### Luminescence and radiocarbon dating results

The sandy aggradation at location IR-7, which is capped by a tufa at  $\pm 20$  m above current stream level, is dated to  $16.8 \pm 1.9$  ka (Figures 5 and 6, Table I). This sediment body thus predates the Kula flow volcanic event (3 ka, Van Gorp *et al.*, 2013) and represents an aggradation phase at the end of the Pleistocene and into the Allerød interstadial (16 ka to 13 ka). The dates also suggest that the muddy deposit at C-1 (13 ka) is younger and thus inset in the sands of IR-7. However, this radiocarbon age estimate has to be used with caution due to the possible

presence of mobile fractions in sample C-1. Since the dates come from the finer upper part of the sediment body, the age of the underlying gravelly aggradation could be significantly older.

Samples IR-8, IR-11 and IR-12 have age estimates between 2.5 and 2.7 ka. This indicates an aggradation phase along a large stretch of the trunk stream. The  $82 \pm 9$  ka of sample IR-9 places this terrace in MIS 5a/b (marine isotope stages). Its age estimate is questionable due to a poor dose recovery. Samples IR-10 and IR-13 exceeded the saturation limits, thus we could only assign minimum age estimates of 140 ka and 173 ka, respectively. Due to unusually high dose rates, these minimum ages are relatively low compared to other feldspar pIRIR-studies (Buylaert *et al.*, 2012).

## Discussion

### Base-level reconstruction

Field interpretations and dating results lead to following chronological reconstruction. Before the first known Middle Pleistocene damming occurred, the Gediz formed a local base level for the Gerén at around 25 m above current river level, suggested by the lowest Gediz terrace at Ar-4. The Gerén Catchment outlet must have been upstream of this location because higher basement ridges just north of Ar-4 confined the Gediz–Gerén confluence. It is not unlikely that this Gerén confluence was even south of its current location (Figure 7A). A main channel within the Gerén Catchment was already located in the centre of the current catchment, evidenced by the largest volume and thickness of limestone gravels and fluvial deposits in the catchment (Figure 3). All these streams were gravel bearing, either with limestone gravels only, or with limestone and Miocene-derived gravels. Damming started at 311 ka (Figure 7B) with the emplacement of flow Ar-4 in the Gediz valley, causing base-level rise to around 40 m above current river level and perhaps forming a lake. Flow Ar-3bottom (274 ka) subsequently entered the valley, but it is unclear if and how this flow dammed the Gediz and Gerén. Subsequently, the Ar-3top flow (240 ka) entered on top of flow Ar-3bottom and possibly into a lake caused by flow Ar-4 (Figure 7C). The duration of these lava dam events is uncertain. The fluvial terrace on top of Ar-4 suggests that the Gediz established a stable course with the lava dam still partly in place, indicating an elevated base level for a prolonged period. Other known lava dams often had fluvial re-establishment on top of the flow or on lake

**Table 1.** Results of pIRIR luminescence,  $^{40}\text{Ar}/^{39}\text{Ar}$  and radiocarbon dating

pIRIR	Lab code	Sample	Location	Altitude (m)	Measurement procedure	Equivalent dose (Gy)	Dose rate (Gy/ka)	Age $\pm 1\sigma$ (ka)	Validity
	NCL-2209135	IR-1 <sup>a</sup>	Below Kula flow	348	Multiple-grain pIRIR <sub>230</sub>	9.2 $\pm$ 0.4	3.0 $\pm$ 0.1	3.0 $\pm$ 0.2	Likely OK
	NCL-2209136	IR-2 <sup>a</sup>	Lower Geren top	378	Multiple-grain pIRIR <sub>230</sub>	12.6 $\pm$ 5.3	2.5 $\pm$ 0.1	5.0 $\pm$ 2.1	Questionable
	NCL-2209137	IR-3 <sup>a</sup>	Lower Geren bottom	372	Multiple-grain pIRIR <sub>230</sub>	22.1 $\pm$ 6.2	2.4 $\pm$ 0.1	9.4 $\pm$ 2.7	Likely OK
	NCL-2209138	IR-7	Lower Geren tufa	390	Multiple-grain pIRIR <sub>231</sub>	50.3 $\pm$ 5.5	3.0 $\pm$ 0.1	16.8 $\pm$ 1.9	Likely OK
	NCL-2111095	IR-8	Geren spa bridge	389	Single-grain pIRIR <sub>150</sub>	5.8 $\pm$ 0.7	2.74 $\pm$ 0.11	2.5 $\pm$ 0.3	Likely OK
	NCL-2111096	IR-9	Geren village terrace	427	multiple grain pIRIR <sub>290</sub>	280 $\pm$ 22	3.40 $\pm$ 0.12	82 $\pm$ 9	questionable, poor dose recorded
	NCL-2111097	IR-10	Aggradation tephra	445	multiple grain pIRIR <sub>290</sub>	$\geq$ 574 $\pm$ 32	4.10 $\pm$ 0.15	$\geq$ 140 $\pm$ 10	in saturation, minimum age
	NCL-2111100	IR-11	Young Geren pottery	429	Single-grain pIRIR <sub>150</sub>	6.7 $\pm$ 0.6	3.18 $\pm$ 0.12	2.5 $\pm$ 0.3	Likely OK
	NCL-2111101	IR-12	Up Geren fluv terrace	451	Single-grain pIRIR <sub>150</sub>	6.1 $\pm$ 0.8	2.78 $\pm$ 0.11	2.7 $\pm$ 0.3	Likely OK
	NCL-2111102	IR-13	Gediz paleomeander	377	multiple grain pIRIR <sub>290</sub>	$\geq$ 572 $\pm$ 53	3.30 $\pm$ 0.12	$\geq$ 173 $\pm$ 15	in saturation, minimum age
$^{40}\text{Ar}/^{39}\text{Ar}$									
	Lab code	Sample	Location	Altitude (m)	K/Ca $\pm 1\sigma$	Normal isochron age $\pm 1\sigma$ (ka)	Inverse isochron age $\pm 1\sigma$ (ka)	Plateau age $\pm 1\sigma$ (ka)	MSWD
	11WG1_C2	Ar-3top		391	0.076 $\pm$ 0.028	256.8 $\pm$ 73.2	257.1 $\pm$ 69.2	240.2 $\pm$ 18.2	0.79
	11WG1_B2	Ar-3bot		391	0.692 $\pm$ 0.072	265.2 $\pm$ 16.1	265.2 $\pm$ 16.1	273.9 $\pm$ 12.8	0.60
	11WG1_B1	Ar-4	Above gravel	372	0.598 $\pm$ 0.113	327.2 $\pm$ 36.5	326.5 $\pm$ 36.6	310.5 $\pm$ 14.8	1.17
$^{14}\text{C}$									
	Sample		Location		$^{14}\text{C}$ age BP (yr)			$1\sigma$ cal BP range (yr)	
	C-1		Lower Geren tufa	380	11400 $\pm$ 45			13290–13230	

<sup>a</sup>These samples already have been described in Van Gorp *et al.* (2013).

Note: MSWD, mean square of weighted deviates.

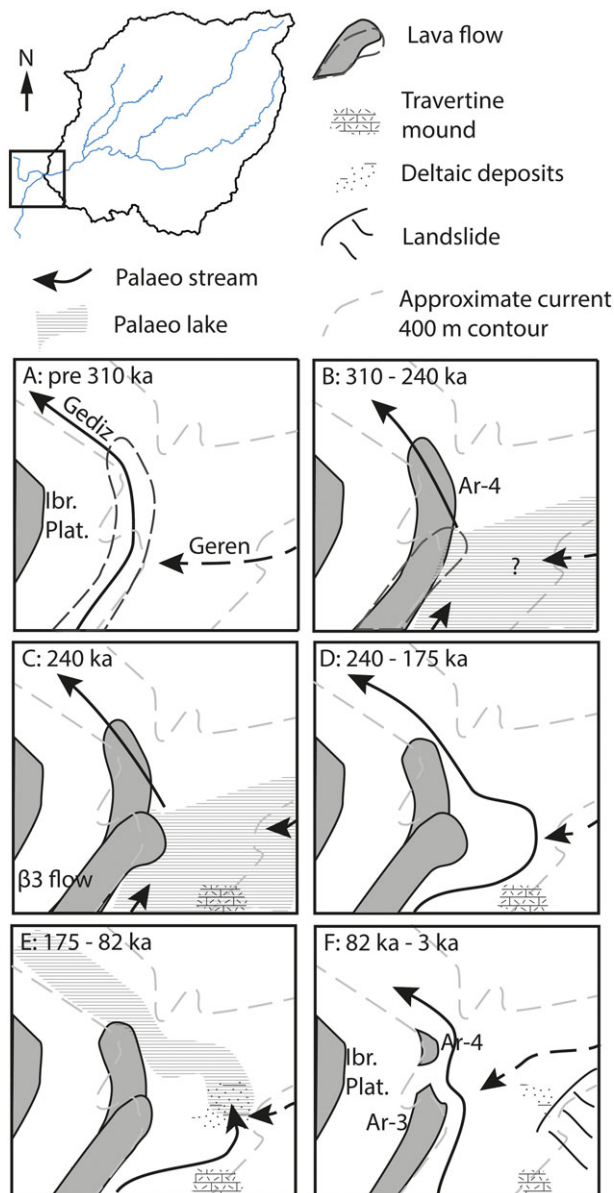


**Figure 7.** Overview and reconstruction of mid Pleistocene to Holocene evolution of the Gediz–Geren confluence [from (A) 310 ka to (E) 3 ka]. This figure is available in colour online at [wileyonlinelibrary.com/journal/esp](http://wileyonlinelibrary.com/journal/esp)

sediments behind the dams (Macaire *et al.*, 1992; Ely *et al.*, 2012), suggesting long dam stability. The Holocene damming by the Kula flow in our study area lasted for 0.5 to 1.2 ka (Van Gorp *et al.*, 2013). The size of this dam is comparable to those of Ar-3 and Ar-4. However re-establishment of a fluvial terrace has not been observed on top of the Kula flow. This suggests that dam duration of the Ar-4 flow has been significantly longer than 1 ka. After lake drainage, the Gediz River re-established itself east of flow Ar-3top (Figure 7D), similar to how the river currently is diverted by the Kula flow (Van Gorp *et al.*, 2013). It was located at terrace IR-13, where a gravelly fluvial terrace resembling a meander bend is preserved around 25 m above current river level. In contrast with the terraces underlying and overlying Ar-4, this terrace is CaCO<sub>3</sub>-cemented, which, assuming relatively arid conditions for such cementation to occur, could link this post-240 ± 18 ka terrace to either the end of MIS 8, MIS 7d stadial or the start of MIS 6 glacial. The deltaic stratified sands and gravels overlying this terrace, which yielded a minimum burial age of 173 ± 15 ka, are not cemented and a damming event reaching at least 285 m a.s.l. may have

been responsible for their deposition. A plausible dam candidate is the lava flow near Palankaya (Figure 1), around 15 km downstream of the Gediz–Geren confluence. The flow overlies a Gediz terrace at 315 m, around 40 m above current river level (Westaway *et al.*, 2004) which, using 0.004 for the average Gediz gradient (Maddy *et al.*, 2012b), corresponds to the altitude of terrace IR-13. An average date of 175 ± 3 ka calculated from three different samples both from the top and the base of the Palankaya flow, indicates that there was a single flow that blocked the Gediz (Westaway *et al.*, 2006). The current top has an elevation of around 390–400 m a.s.l. where it has blocked the river. The volume of the lava that flowed into the river valley is significant (roughly estimated valleyfill of ~0.1 km<sup>3</sup>) and could have created a lake all the way up into the Geren Catchment. It is unclear if the lake was filled up all the way to the top of the lava dam, but a base-level rise affecting the Geren–Gediz confluence area is likely and corresponds both in elevation and timing with the deltaic sediments at IR-13 (Figure 7E). The duration of the Palankaya dam could have been significant, up to several 10 ka, given its volume. However, in between the Gediz–Geren confluence and Palankaya, 15 km downstream, no clear evidence of lake sediments has been observed. A possible reason for this absence of lake sediments is that upstream, the Gediz may have been still been dammed by the Söğüt lava flow, dated to 236 ± 6 ka at its most upstream edge (Westaway *et al.*, 2006; Figure 1), which formed another large lava dam and could have trapped most of the fine sediments. Furthermore, damming by the Palankaya flow would also have blocked the Selendi catchment to the north (Figure 1) which could have involved the storage of considerable amounts of water. The southern slopes of the Gediz–Geren confluence and the gorge area between the Gediz–Geren confluence and the Gediz–Selendi confluence show signs of fossil and active landsliding and mass movements. Lake sediments may therefore either have been removed or obscured. It is possible that lake formation and subsequent dam removal has destabilized slopes more than they would have been from an incising river only and that landslides were most active along the former lake shore area. The fluvial terrace dated to 82 ka (MIS 5a), at 30 m above current river level, suggests that the Geren trunk stream did not incise much until 90 ka after Palankaya dam formation, suggesting a long lasting impact of the Palankaya dam on base level. Associated with this 310–82 ka damming period are two travertines, one south of the Gediz–Geren confluence (Figure 3 and 7) and one near sample IR-9 (Figure 3), suggested by their landscape position and both their tops. The latter one has an unpublished uranium-thorium dating (U-Th) age estimate from 121 to 118 ka at its base (Candy, personal communication 30–01–2012). Interestingly, the large landslide from the Sarnic plateau appears to be contemporaneous with or later than IR-13 and its emplacement could have had major impact on the Geren base level as well and may have pushed the Geren stream to its current position. Meanwhile, the Gediz migrated back west and attained its position prior to eruption of the Kula lava flow (Figure 7F). For further details on Gediz response to the Holocene damming, the reader is referred to Van Gorp *et al.* (2013).

In summary, three different lava flows which have dammed the Geren Catchment from 310.5 ka to 175 ka have been recognized. However, damming durations are uncertain and climate change is also an important driver for incision–aggradation cycles. Their relative impact on the evolution of the Geren Catchment is not yet clear. LEM simulations were intended to help answer this question. Before discussing and interpreting the field results of the more upstream parts of the Geren Catchment, the base-level reconstruction is translated into a model input and other LEM scenario inputs and results are presented.

## Model inputs and scenarios

Model setup and calibrated parameters from Van Gorp *et al.* (2015) were used as a starting point for the current study. Three main inputs have been used for modelling: the palaeo-DEM a climate record influencing effective rainfall, and a base-level change record (Figure 7).

Effective rainfall was derived from the Tenaghi Phillipon arboreal pollen (%AP) record (Tzedakis *et al.*, 2003, 2006), which is the closest and most complete record spanning our 300 ka timescale. An annual record was created using linear interpolation. For simplicity, effective rainfall was linearly scaled from the arboreal pollen record around an average effective rainfall of  $50 \text{ mm a}^{-1}$  (Figure 7B), which is the constant rainfall used by Van Gorp *et al.* (2015) and is a methodology analogous to Stemerink *et al.* (2010).

Vegetation feedbacks are important for landscape evolution (Istanbulluoglu and Bras, 2005; Macklin and Lewin, 2008; Veldkamp *et al.*, 2015). A climate-driven vegetation effect is incorporated in the model by scaling erodibility factor  $K$  and sedimentation factor  $P$ . According to the %AP record, vegetation cover has been varying between tree-domination and shrub-domination. For effective rainfall over  $50 \text{ mm}$ ,  $K$  was lowered by 25% due to vegetation stabilizing the soil. The value of  $P$  was increased by 25% due to vegetation being able to capture more sediments. If effective rainfall is lower than  $50 \text{ mm}$ , erodibility factor  $K$  is increased by 25% due to less vegetation stabilizing the soil. Sedimentation factor  $P$  is increased by 25% due to the decrease in potential capture by vegetation. This reflects a first-order influence of rainfall on vegetation cover (%AP, Tzedakis *et al.*, 2006) and is a simplified version of how the effect of vegetation on erosion was incorporated by Temme *et al.* (2009).

As mentioned, the initial base level of the catchment was set to  $390 \text{ m}$ . Base level change was imposed on the first 210 m (seven columns) of gridcells at the outlet (Figure 8A). With  $390 \text{ m}$  as a start outlet cell elevation, three scenarios of base-level change are imposed on the catchment. The first scenario is gradual base-level lowering according to the known average incision of the Gediz River of  $0.14 \text{ mm a}^{-1}$  (Maddy *et al.*, 2012b). In the second and third base-level scenario, damming events are added, corresponding to the observed events at 310, 274, 240, 175 and 3 ka (Table II). Their elevations are approximated from corresponding lava tops. Their emplacement and removal occurs in one timestep and is imposed rather than simulated by the model. Given that the work to remove dams is done by the Gediz River rather than the Geren, while it is Geren Catchment evolution that is modelled, we consider this is an acceptable assumption. In the second scenario, damming durations were 1 ka, based on the maximum age-constrained damming duration of around 1 ka of the Kula flow (Van Gorp *et al.*, 2013, 2015). The Palankaya dam (175 ka) was given a five times longer duration based on its approximately five times wider dam. However, as discussed earlier, durations of the older lava dams are not directly age constrained.

Due to this uncertainty of dam duration, and given the field indications that the Gediz flowed over the Ar-4 dam for a longer period and that the Geren trunk stream did not incise much until around 82 ka, we used a third base-level scenario with longer dam durations (Table II). In this third scenario dams from 0 yr. (300 ka) to 59 800 yr. (240.2 ka) form a stable and finally increased base level (Figure 8B) and the Palankaya dam has a duration of 50 000 yr.

LAPSUS was run for 300 000 yr. for all three scenarios. Results were assessed by monitoring the evolution of 1 ka-averaged elevations of a downstream trunk stream

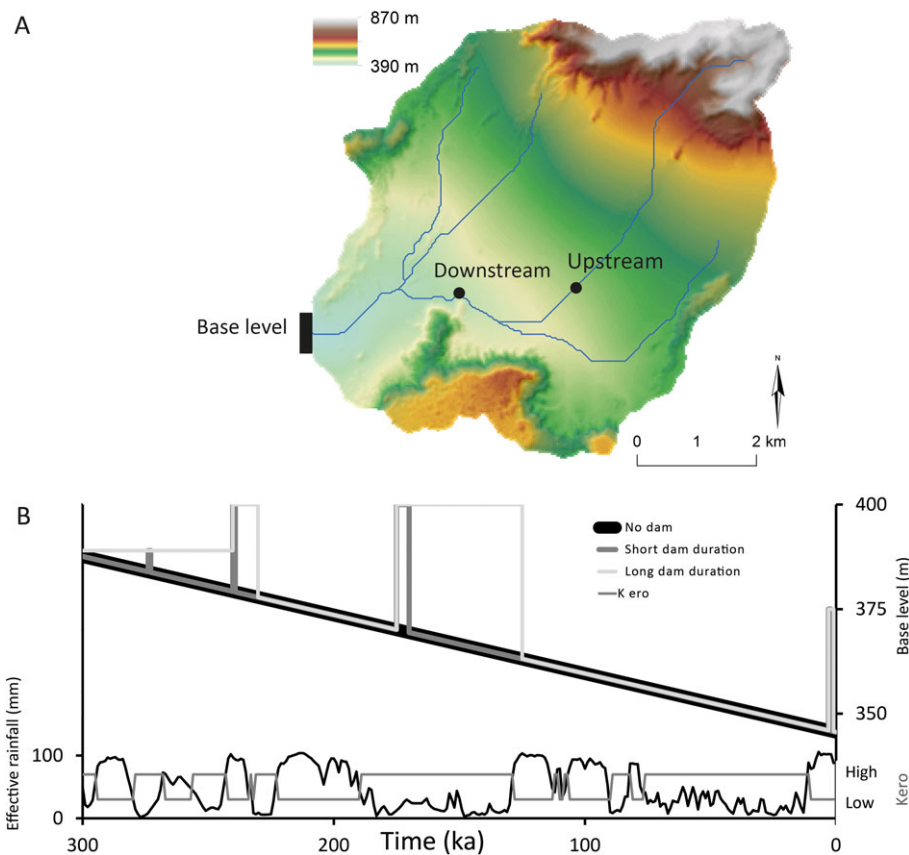


**Figure 8.** Main model inputs with: (A) palaeo-DEM with drainage network, the area of which base level was changed, and tracked channel locations are indicated; (B) field-derived base-level change without, with short and with long duration dams, effective rainfall input and erodibility factor. This figure is available in colour online at [wileyonlinelibrary.com/journal/espl](http://wileyonlinelibrary.com/journal/espl)

**Table II.** Dates and durations of dam events for the long and short-dam-duration scenarios

Age (ka)	Simulation time (yr)	Dam number	Elevation	Dam duration (yr)		Based on
				Short	Long	
300	0	1	390	Gradual incision	59800	This study
273.9	26100	2	390	1000	—	This study
240.2	59800	3	400	1000	10000	This study
175	125000	4	400	10000	50000	Westaway <i>et al.</i> (2006)
3	297000	5	375	900	2000	Van Gorp <i>et al.</i> (2013)

location, at the location of sample IR-9 and an upstream trunk stream location, at the location of sample IR-10 (Figure 8A).

### Model results: climate change versus damming events

The results of 300 000 yr. simulation of upstream and downstream channel elevation show different pathways (Figure 9). Upstream evolution shows a top-down control, where incision generally occurs in low rainfall periods due to low sediment load but sufficient incision power in the trunk streams, and aggradation or hampered incision in high rainfall periods due to high sediment supply when transport capacity is often exceeded. This image qualitatively matches sediment accumulation rates derived from the Tenaghi Phillipon record, which are also higher during inter-glacials (Tzedakis *et al.*, 2003). For all three scenarios, the upstream channel location first incises and then becomes relatively stable around 20 000 yr. (Figure 9). From then on, alternating incision and aggradation phases can be observed, varying in length from 1000 yr. to over 50 000 yr.

However, downstream evolution in all three scenarios is largely controlled by base-level change (bottom-up control). Downstream channel elevation starts with a long relatively stable phase until 75 000 yr., which is probably due to continuously high sediment load. The downstream reach of the long-dam-duration scenario has a sustained stable level until 10 000 yr. after the Palankaya dam was removed. Visual correlation of aggradation and incision phases in these downstream locations with climate is weak (Figure 10), although the no-dams scenario perhaps is sensitive to 100 ka cycles, showing increased alternating activity. However, the complexity of the erosion signal is high. Visual correlation with rainfall of these phases in both dam scenarios is even weaker, suggesting their dampening influence on climate signals (Veldkamp and Tebbens, 2001).

The no-dam scenario shows a wave of incision and equally high aggradation in MIS 6, between 125 000 yr. and 175 000 yr. of simulation. Timing of this large-scale incision–aggradation phase is similar for upstream and downstream reaches. In the short-dam-duration scenario, this incision wave is delayed. In the long-dam-duration scenario, upstream incision is delayed until around 250 000 yr., after which continuous incision occurs. Downstream incision is delayed and occurs more gradual in the period from 180 000 to 285 000 yr. In the no-dam and short-dam-duration scenario, net incision is limited in this period. With the increase of rainfall at the end of the Pleistocene, the long-dam-duration scenario responds directly by channel aggradation, while the no-dams and short-dam-duration scenarios do not. These differences suggest a long-term complex response to the Middle Pleistocene damming events. The last dam shows a relatively minor impact on trunk stream evolution, which is already coping with increased sediment supply. However, continued long-term response to this recent damming event into the future is likely.

Modelling thus simulates an increasing influence of damming events on incision aggradation patterns, which obscures the already complex link of incision patterns with climate change even more. Interpreting them in concert with obtained fieldwork results increases our understanding of both history of and mechanisms in the Geren Catchment.

The >50 m incision and subsequent >50 m aggradation simulated in the no-dam and short-dam-duration scenarios during MIS 6 to 5 are not observed in the field, which makes their validity highly unlikely. However, the long-dam-duration scenario demonstrates delayed incision until MIS 5, followed by aggradation–incision cycles from MIS 5 to the end of the Pleistocene of the same order of magnitude as those observed in the field. This scenario thus reproduces Geren evolution best and will be used for further field-model integration.

### Field–model integration: 300–82 ka landscape evolution of the Geren Catchment

In the upstream channel, at IR-10, the CaCO<sub>3</sub>-cemented terrace around 20–30 m above current stream level, which is overlain by an uncemented aggradation of fine-grained deposits, indicates a significant regime shift and it is probable that the aggradation at IR-10 is contemporary with the 310–175 ka damming events and more specifically with the deltaic aggradation found at IR-13 at the Gediz–Geren confluence.

Because we only obtained a lower age boundary, these aggradations could have been synchronous with the Middle Pleistocene damming phase. However, climate-driven major aggradational phases in catchments of the Mediterranean basin have been recognized in the middle and late Pleistocene, although data coverage is still limited (Macklin *et al.*, 2002). Nevertheless, an aggradation phase in MIS 6 is recognized by Macklin *et al.* (2002), while a Pre-MIS 5 aggradation is suggested from samples IR-10 and IR-13. The long-dam-duration scenario suggests that this upstream >140 ka channel aggradation took place in MIS 6 or 7 and is at least partly climate-driven.

### Field model integration: post-dam landscape evolution

From fieldwork it is unknown when the aggradation associated with sample IR-10 and IR-13 ended. The age and elevation of fill terrace IR-9 of 82 ka suggests that post-175 ka, incision of the Geren trunk stream has been limited throughout MIS 6 and 5. It must be noted that the elevation of the downstream 82 ka dated deposits of IR-9 is higher than channel elevation of the long-dam-duration scenario, which could be caused both by dating uncertainty or model uncertainty. Noting the questionable validity of the age of IR-9, the burial age itself falls in MIS 5a/b, which has already been mentioned as a climate-driven fluvial deposition phase in the Mediterranean (Macklin

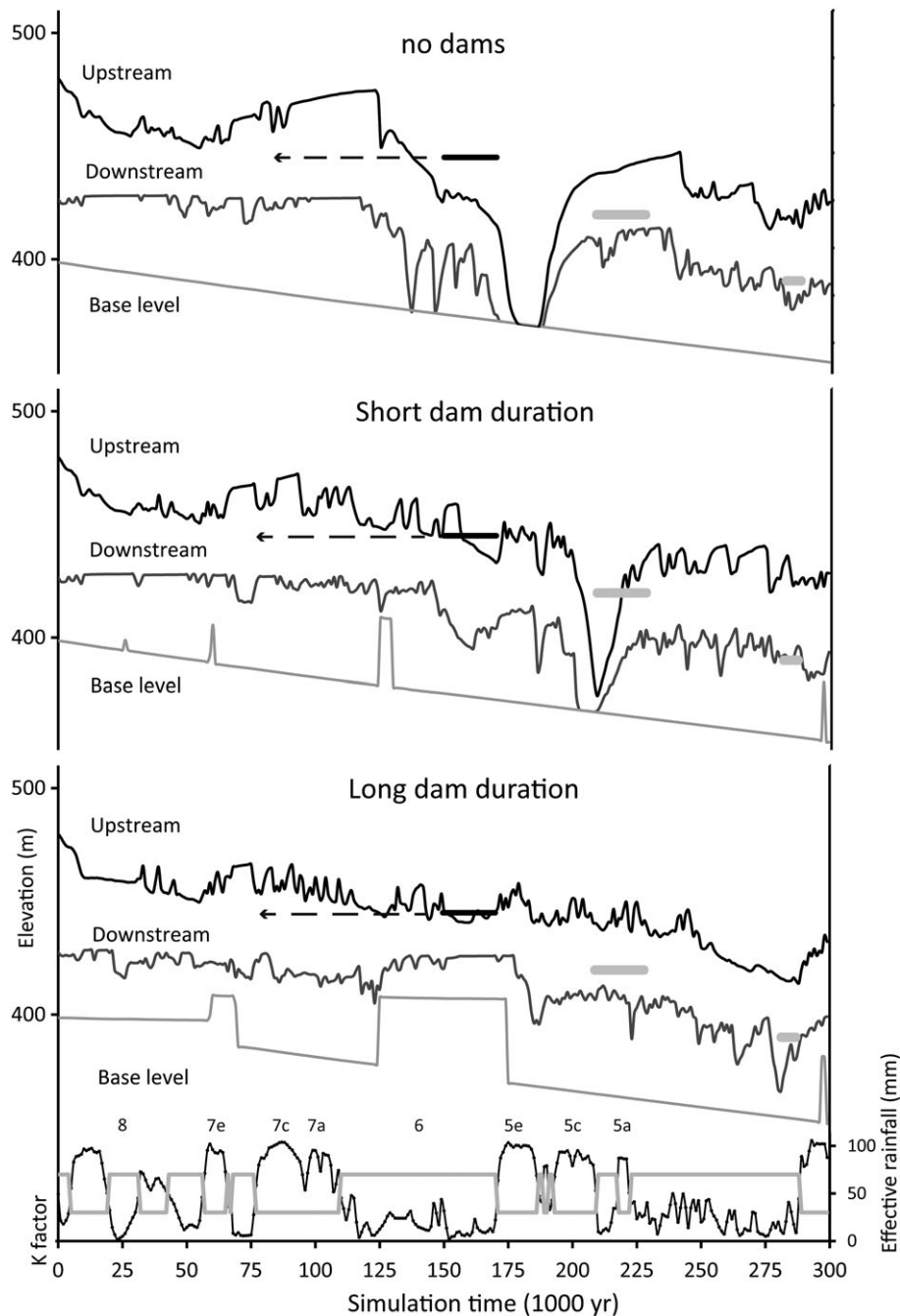


**Figure 9.** Model output showing 1000 yr. averaged channel elevation development at an upstream and downstream location within the trunk stream for the 'no-dam', 'short-dam-duration' and 'long-dam-duration' scenarios'. Imposed base-level change and age estimates of fluvial deposits of up and downstream locations are plotted as thick horizontal bars for comparison (upstream: IR-10 with dotted arrows indicating minimum age; downstream: IR-9 and IR-7). Bottom part shows for reference the percentage arboreal pollen (%AP) of the last 300 ka of Tenaghi Phillipon which is used as a climate input, in grey, the alternation of high and low *K*-factors is shown, see text for explanation. Some marine isotope stages (MIS) are indicated.

*et al.*, 2002). During subsequent incision of around 35 m, no significant terraces have been found. Probably, confinement of channels in this period caused a lack of preservation potential. The end of this incision phase is not specified, but maximum incision to around 3–5 m above current stream level is reached at the base of the fluvial deposits at location IR-7. This incision phase is also simulated and ends around 282 000 yr. (18 ka) in the downstream channel and around 288 000 yr. (12 ka) in the upstream channel. Thus a downstream aggradation phase is already initiated but has not yet reached the elevations which follow from the dated sediments of IR-7 in the downstream reach. At this location the basal fluvial gravel aggradation phase is not dated, but its lower age is constrained by the fine sands covering it and which are dated to 16.8 ka.

This simulated aggradation phase seems overestimated and subsequent channel incision leading to the presently observed stream form is not reproduced by the model. This incision of approximately 20 m occurs between 16.8 and 9.2 ka, when deposition starts at location IR-3. A final deposition phase occurs along the whole length of the trunk stream around 2.5 ka, after which incision to the current stream level is established. This final aggradation occurs synchronously with the Holocene damming event, suggesting that it is a backfilling response to this event. The downstream deposits of IR-3 have already been correlated to the 3 ka damming event (Van Gorp *et al.*, 2013) and location IR-8, which consists of an 8 m sandy fining upward sequence, may indicate a response to damming. Those samples from further upstream, IR-11 and IR-12, are coarse sandy and

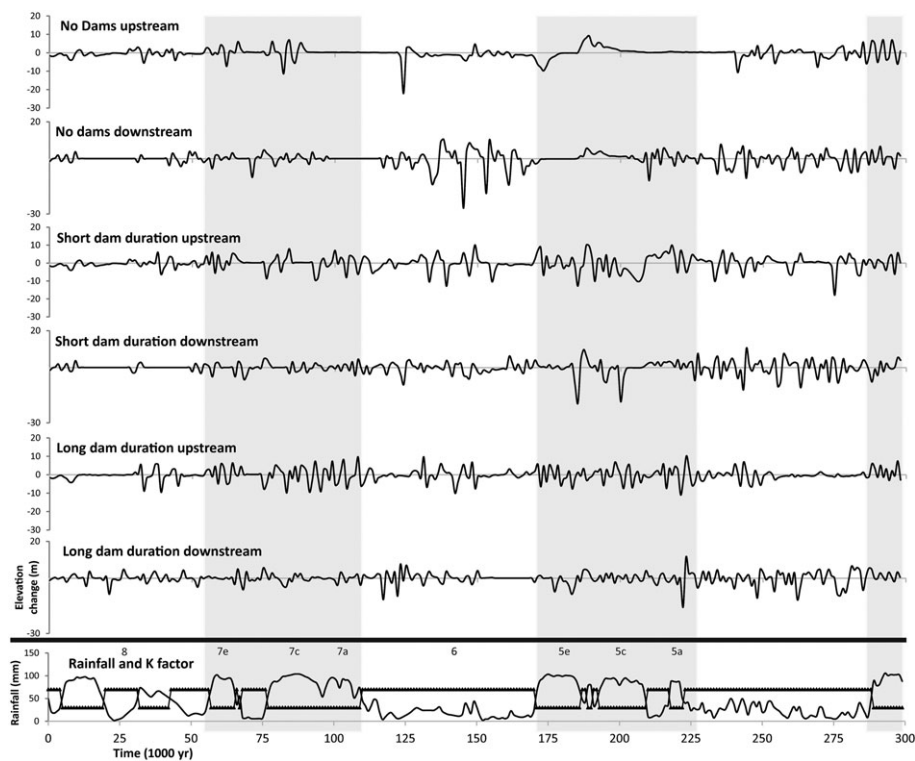


**Figure 10.** Simulation output of 1000 yr. averaged erosion and deposition amounts (in metres) of the three scenarios at upstream and downstream channel locations. Rainfall, *K* factor variation (no scale) and MIS are added for comparison.

gravelly aggradations, where IR-11 resembles a fluvial channelfill which is probably driven by sediment supply, and IR-12 contains pottery, indicating contemporaneous human activity and its potential impact on erosion.

In summary, fieldwork and dating clarified that the Gediz–Geren outlet area experienced multiple damming events, which are contemporary with aggradation–incision phases in the Geren. Landscape evolution modelling demonstrated that imposing long-duration damming events reproduce the general evolution of the catchment best. Modelling and field reconstruction both show how base-level has been relatively stable for a prolonged period, after which there was an incision phase lasting until the Holocene. Apparently, when evidence for such a prolonged stable base level is found, long-duration dams are a possible cause. Fluvial terraces and stream aggradations are still linked to periods with high rainfall (cf. Bridgland and Westaway, 2014), even in a small catchment such as the Geren. However, their preservation and relative elevation obscures this link due to catchment complexity (cf. Jerolmack and Paola, 2010) and its specific history, in this case lava damming events.

### Model validity

The model studies presented in this paper simplify and compromise some processes that play an important role in reality. For instance, timing of damming events in relation to prevailing climate may have been an additional factor determining dam duration. The Palankaya dam (175 ka) coincided with the dry conditions of MIS 6, which could have delayed lake infilling, siltation and subsequent erosion by overtopping. Landsliding will have had a significant impact on catchment evolution and its incorporation in future of this type is recommended, as the effect may have been felt throughout the Geren Catchment (cf. Temme *et al.*, 2011). Probable reasons for the model failing to reproduce the most recent aggradation–incision

history could be the lack of these landslide effects, a divergence of the 300 ka simulated DEM from the actual Late Pleistocene topography, and, for the late Holocene, human impact of land use–land cover change. A sensitivity or uncertainty analysis of input parameters may be desired to strengthen model results.

Nevertheless, by keeping input parameters relatively simple, we already demonstrate that model results suggest long-duration dams, and demonstrate the complexity of spatial catchment evolution under simple changing driving conditions. The suggested long damming durations provide testable hypotheses for further fieldwork research. For instance we could test the hypothesis that the landslide at the Gediz–Geren confluence contributed significantly to long duration damming, or the hypothesis that the Palankaya lava dam was long-lived. The addition of climate change to the simulations with respect to the stable-climate simulations by Van Gorp *et al.* (2015), allowed us to acknowledge that the link between terrace formation and climate change still exists but is obscured. Although in our model output, preservation of terraces only occurred near the dam location and not in confined channels, major aggradation–incision cycles within the confined channels are presumed to represent potential terraces that can be preserved within the actual streams and which could now be better recognized in the field. Late Pleistocene–Holocene evolution until present could be further investigated using a more detailed Late Pleistocene–Holocene palaeo-DEM, a more detailed climate–landcover input and a more detailed version of LEM LAPSUS (cf. Temme and Veldkamp, 2009; Baartman *et al.*, 2012).

### Conclusion

A combined fieldwork, dating and landscape evolution modelling study of Middle Pleistocene to Holocene evolution of the Geren Catchment, western Turkey, demonstrates that there have been at least three Middle Pleistocene damming events

downstream of the Gediz–Geren confluence. Modelling showed that long-duration Middle Pleistocene lava dams can explain the observed hampered incision and subsequent incision–aggradation cycles. Dated fluvial deposits are linked with climate forcing but the generally observed uplift-driven stepped terraces are not present due to damming events. Furthermore, catchment response differs between upstream and downstream locations and its evolution is complex. To better simulate Late Pleistocene evolution until present, it is suggested that a more detailed LEM simulation should be performed, which takes the most recent human induced landcover changes into account. Combined field–LEM studies such as this one are useful in unravelling spatially explicit feedbacks and will enhance our understanding of landscapes compared to either fieldwork or modelling studies alone.

**Acknowledgements**—Luminescence dating was funded by investment grant (#834.03.003) supplied by the Netherlands organization for scientific research (NWO–ALW). Comments by David Bridgland and an anonymous reviewer greatly improved this manuscript.

## References

- Baartman JEM, Temme AJAM, Schoorl JM, Braakhekke MH, Veldkamp TA. 2012. Did tillage erosion play a role in millennial scale landscape development? *Earth Surface Processes and Landforms* **37**: 1615–1626.
- Bridgland DR, Westaway R. 2014. Quaternary fluvial archives and landscape evolution: a global synthesis. *Proceedings of the Geologists' Association* **125**: 600–629. DOI:10.1016/j.pgeola.2014.10.009.
- Buylaert JP, Jain M, Murray AS, Thomsen KJ, Thiel C, Sohbati R. 2012. A robust feldspar luminescence dating method for Middle and Late Pleistocene sediments. *Boreas* **41**: 435–451.
- Capra L. 2007. Volcanic natural dams: identification, stability, and secondary effects. *Natural Hazards* **43**: 45–61.
- Crow R, Karlstrom KE, McIntosh W, Peter L, Dunbar N. 2008. History of Quaternary volcanism and lava dams in western Grand Canyon based on lidar analysis,  $^{40}\text{Ar}/^{39}\text{Ar}$  dating, and field studies: implications for flow stratigraphy, timing of volcanic events, and lava dams. *Geosphere* **4**: 183–206. DOI:10.1130/ges00133.1.
- Ely LL, Brossy CC, House PK, Safran EB, O'Connor JE, Champion DE, Fenton CR, Bondre NR, Orem CA, Grant GE, Henry CD, Turrin BD. 2012. Owyhee River intracanyon lava flows: does the river give a dam? *Bulletin of the Geological Society of America* **124**: 1667–1687.
- Ermini L, Casagli N. 2003. Prediction of the behaviour of landslide dams using a geomorphological dimensionless index. *Earth Surface Processes and Landforms* **28**: 31–47.
- Foster GR, Meyer LD. 1972. A closed-form soil erosion equation for upland areas. In *Sedimentation: Symposium to Honour Professor H.A. Einstein*, Shen HW (ed). Colorado State University: Fort Collins, CO; 190–207.
- Foster GR, Meyer LD. 1975. Mathematical simulation of upland erosion by fundamental erosion mechanics. In *Proceedings, Sediment-yield Workshop, Present and Prospective Technology for Predicting Sediment Yields and Sources*. USDA Sedimentation Laboratory: Oxford, MS; 190–207.
- Freeman TG. 1991. Calculating catchment area with divergent flow based on a regular grid. *Computers and Geosciences* **17**: 413–422.
- Gotttdang A, Mous DW, Van der Plicht J. 1995. The HVEE (super 14) C system at Groningen. *Radiocarbon* **37**: 649–656.
- Istanbulluoglu E, Bras RL. 2005. Vegetation-modulated landscape evolution: effects of vegetation on landscape processes, drainage density, and topography. *Journal of Geophysical Research: Earth Surface* **110**: F02012. DOI:10.1029/2004JF000249.
- Jerolmack DJ, Paola C. 2010. Shredding of environmental signals by sediment transport. *Geophysical Research Letters* **37**(19). DOI:10.1029/2010GL044638.
- Kars RH, Busschers FS, Wallinga J. 2012. Validating post IR-IRSL dating on K-feldspars through comparison with quartz OSL ages. *Quaternary Geochronology* **12**: 74–86.
- Kaufman DS, O'Brien G, Mead JI, Bright J, Umhoefer P. 2002. Late Quaternary spring-fed deposits of the Grand Canyon and their implication for deep lava-dammed lakes. *Quaternary Research* **58**: 329–340.
- Kirkby MJ. 1971. Hillslope process-response models based on the continuity equation. In *Slopes, Forms and Processes*. Transactions of the IBG. Special Publication, Brunsden D (ed). Royal Geographical Society: London; 15–30.
- Koppers AAP. 2002. ArArCALC–software for  $^{40}\text{Ar}/^{39}\text{Ar}$  age calculations. *Computers and Geosciences* **28**: 605–619.
- Korup O, Tweed F. 2007. Ice, moraine, and landslide dams in mountainous terrain. *Quaternary Science Reviews* **26**: 3406–3422.
- Korup O, Strom AL, Weidinger JT. 2006. Fluvial response to large rock-slope failures: examples from the Himalayas, the Tien Shan, and the Southern Alps in New Zealand. *Geomorphology* **78**: 3–21.
- Macaire JJ, Cocirca C, De Luca P, Gay I, DeGoer De Herve A. 1992. Origins, ages and evolution of the tardi- and postglacial lacustrine systems in the 'lac Chambon' basin, Puy-de-Dome, France. *Comptes Rendus – Academie des Sciences, Serie II* **315**: 1119–1125.
- Macklin MG, Fuller IC, Lewin J, Maas GS, Passmore DG, Rose J, Woodward JC, Black S, Hamlin RHB, Rowan JS. 2002. Correlation of fluvial sequences in the Mediterranean basin over the last 200 ka and their relationship to climate change. *Quaternary Science Reviews* **21**(14–15): 1633–1641.
- Macklin MG, Lewin J. 2008. Alluvial responses to the changing earth system. *Earth Surface Processes and Landforms* **33**: 1374–1395. DOI:10.1002/esp.1714.
- Maddy D, Demir T, Bridgland DR, Veldkamp A, Stemerink C, van der Schriek T, Schreve D. 2007. The Pliocene initiation and early Pleistocene volcanic disruption of the palaeo-Gediz fluvial system, western Turkey. *Quaternary Science Reviews* **26**: 2864–2882.
- Maddy D, Veldkamp A, Jongmans AG, Candy I, Demir T, Schoorl JM, van der Schriek T, Stemerink C, Scaife RG, van Gorp W. 2012a. Volcanic disruption and drainage diversion of the palaeo-Hudud River, a tributary of the Early Pleistocene Gediz River, western Turkey. *Geomorphology* **165–166**: 62–77. DOI:10.1016/j.geomorph.2011.12.032.
- Maddy D, Demir T, Veldkamp A, Bridgland DR, Stemerink C, van der Schriek T, Schreve D. 2012b. The obliquity-controlled early Pleistocene terrace sequence of the Gediz river, western Turkey: a revised correlation and chronology. *Journal of the Geological Society* **169**: 67–82. DOI:10.1144/0016-76492011-011.
- Maddy D, Schreve D, Demir T, Veldkamp A, Wijbrans JR, van Gorp W, van Hinsbergen DJJ, Dekkers MJ, Scaife R, Schoorl JM, Stemerink C, van der Schriek T. 2015. The earliest securely-dated hominin artefact in Anatolia? *Quaternary Science Reviews* **109**: 68–75. DOI:10.1016/j.quascirev.2014.11.021.
- O'Connor JE, Beebe RA. 2009. Floods from natural rock-material dams. In *Mega-floods on Earth and Mars*, Burr D, Carling P, Baker V (eds). Cambridge University Press: Cambridge; 128–171.
- O'Connor JE, Clague JJ, Walder JS, Manville V, Beebe RA. 2013. Outburst Floods. In *Treatise on Geomorphology*, volume 9 (Fluvial Geomorphology), Wohl EE (ed). Academic Press: San Diego, CA; 475–510. Shroder J (Editor in Chief)
- Pedley M, González Martín JA, Ordóñez Delgado S, García Del Cura MÁ. 2003. Sedimentology of quaternary perched springline and paludal tufas: criteria for recognition, with examples from Guadalajara Province, Spain. *Sedimentology* **50**: 23–44.
- Purvis M, Robertson A. 2004. A pulsed extension model for the Neogene–Recent E–W-trending Alasehir Graben and the NE–SW-trending Selendi and Gordes basins, western Turkey. *Tectonophysics* **391**: 171–201.
- Quinn P, Beven K, Chevallier P, Planchon O. 1991. The prediction of hillslope flow paths for distributed hydrological modelling using digital terrain models. *Hydrological Processes* **5**: 59–79.
- Reimann T, Tsukamoto S, Naumann M, Frechen M. 2011. The potential of using K-rich feldspars for optical dating of young coastal sediments – a test case from Darss-Zingst Peninsula (southern Baltic Sea coast). *Quaternary Geochronology* **6**: 207–222.
- Reimann T, Thomsen KJ, Jain M, Murray AS, Frechen M. 2012. Single-grain dating of young sediments using the pIRIR signal from feldspar. *Quaternary Geochronology* **11**: 28–41.
- Reimann T, Tsukamoto S. 2012. Dating the recent past (< 500 years) by post-IR IRSL feldspar – examples from the North Sea and Baltic Sea coast. *Quaternary Geochronology* **10**: 180–187.



- Reimer PJ, Baillie MGL, Bard E, Bayliss A, Warren Beck J, Bertrand CJH, Blackwell PG, Buck CE, Burr GS, Cutler KB, Damon PE, Lawrence Edwards R, Fairbanks RG, Friedrich M, Guilderson TP, Hogg AG, Hughen KA, Kromer B, McCormac G, Manning S, Ramsey CB, Reimer RW, Remmele S, Southon JR, Stuiver M, Talamo S, Taylor FW, van der Plicht J, Weyhenmeyer CE. 2004. IntCal04 terrestrial radiocarbon age calibration, 0–26 cal kyr BP. *Radiocarbon* **46**: 1029–1058.
- Richardson-Bunbury JM. 1996. The Kula volcanic field, western Turkey: the development of a Holocene alkali basalt province and the adjacent normal-faulting graben. *Geological Magazine* **133**: 275–283.
- Roach IC, Hill SM, Lewis AC. 2008. Evolution of a small intraplate basaltic lava field: Jerrabattgulla creek, upper shoalhaven river catchment, southeast New South Wales. *Australian Journal of Earth Sciences* **55**: 1049–1061. DOI:10.1080/08120090802266543.
- Schoorl JM, Sonneveld MPV, Veldkamp A. 2000. Three-dimensional landscape process modelling: the effect of DEM resolution. *Earth Surface Processes and Landforms* **25**: 1025–1034.
- Schoorl JM, Veldkamp A, Bouma J. 2002. Modeling water and soil redistribution in a dynamic landscape context. *Soil Science Society of America Journal* **66**: 1610–1619.
- Schoorl JM, Boix Fayos C, De Meijer RJ, Van Der Graaf ER, Veldkamp A. 2004. The 137Cs technique applied to steep Mediterranean slopes (Part II): landscape evolution and model calibration. *Catena* **57**: 35–54.
- Schoorl JM, Veldkamp A, Claessens L, van Gorp W, Wijbrans JR. 2014a. Edifice growth and collapse of the Pliocene Mt. Kenya: evidence of large scale debris avalanches on a high altitude glaciated volcano. *Global and Planetary Change* **123**: 44–54. DOI:10.1016/j.gloplacha.2014.10.010.
- Schoorl JM, Temme AJAM, Veldkamp T. 2014b. Modelling centennial sediment waves in an eroding landscape – catchment complexity. *Earth Surface Processes and Landforms* **39**: 1526–1537. DOI:10.1002/esp.3605.
- Seyitoglu G. 1997. Late Cenozoic tectono-sedimentary development of the Selendi and Uşak-Güre basins: a contribution to the discussion on the development of east–west and north trending basins in western Turkey. *Geological Magazine* **134**: 163–175.
- Stemerdink C, Maddy D, Bridgland DR, Veldkamp A. 2010. The construction of a palaeodischarge time series for use in a study of fluvial system development of the Middle to Late Pleistocene Upper Thames. *Journal of Quaternary Science* **25**: 447–460.
- Temme AJAM, Schoorl JM, Veldkamp A. 2006. Algorithm for dealing with depressions in dynamic landscape evolution models. *Computers and Geosciences* **32**: 452–461.
- Temme AJAM, Baartman JEM, Schoorl JM. 2009. Can uncertain landscape evolution models discriminate between landscape responses to stable and changing future climate? A millennial-scale test. *Global and Planetary Change* **69**: 48–58.
- Temme AJAM, Veldkamp A. 2009. Multi-process Late Quaternary landscape evolution modelling reveals lags in climate response over small spatial scales. *Earth Surface Processes and Landforms* **34**: 573–589.
- Temme AJAM, Claessens L, Veldkamp A, Schoorl JM. 2011. Evaluating choices in multi-process landscape evolution models. *Geomorphology* **125**: 271–281. DOI:10.1016/j.geomorph.2010.10.007.
- Thomsen KJ, Murray AS, Jain M, Bøtter-Jensen L. 2008. Laboratory fading rates of various luminescence signals from feldspar-rich sediment extracts. *Radiation Measurements* **43**: 1474–1486.
- Tzedakis PC, McManus JF, Hooghiemstra H, Oppo DW, Wijmstra TA. 2003. Comparison of changes in vegetation in northeast Greece with records of climate variability on orbital and suborbital frequencies over the last 450 000 years. *Earth and Planetary Science Letters* **212**: 197–212. DOI:10.1016/s0012-821x(03)00233-4.
- Tzedakis PC, Hooghiemstra H, Pälike H. 2006. The last 1.35 million years at Tenaghi Philippon: revised chronostratigraphy and long-term vegetation trends. *Quaternary Science Reviews* **25**: 3416–3430.
- Van Gorp W, Veldkamp A, Temme AJAM, Maddy D, Demir T, Van der Schriek T, Reimann T, Wallinga J, Wijbrans J, Schoorl JM. 2013. Fluvial response to Holocene volcanic damming and breaching in the Gediz and Geren Rivers, western Turkey. *Geomorphology* **201**: 430–448. DOI:10.1016/j.geomorph.2013.07.016.
- Van Gorp W, Temme AJAM, Baartman JEM, Schoorl JM. 2014. Landscape evolution modelling of naturally dammed rivers. *Earth Surface Processes and Landforms* **39**: 1587–1600. DOI:10.1002/esp.3547.
- Van Gorp W, Temme AJAM, Veldkamp A, Schoorl JM. 2015. Modelling long-term (300 ka) upland catchment response to multiple lava damming events. *Earth Surface Processes and Landforms* **40**: 888–900. DOI:10.1002/esp.3689.
- Veldkamp A, Tebbens LA. 2001. Registration of abrupt climate changes within fluvial systems: Insights from numerical modelling experiments. *Global and Planetary Change* **28**: 129–144.
- Veldkamp A, Schoorl JM, Wijbrans JR, Claessens L. 2012. Mount Kenya volcanic activity and the Late Cenozoic landscape reorganisation in the upper Tana fluvial system. *Geomorphology* **145–146**: 19–31.
- Veldkamp A, Candy I, Jongmans AG, Maddy D, Demir T, Schoorl JM, Schreve D, Stemerdink C, van der Schriek T. 2015. Reconstructing Early Pleistocene (1.3 Ma) terrestrial environmental change in western Anatolia: did it drive fluvial terrace formation? *Palaeogeography, Palaeoclimatology, Palaeoecology* **417**: 91–104. DOI:10.1016/j.palaeo.2014.10.022.
- Wallinga J, Bos AJJ, Dorenbos P, Murray AS, Schokker J. 2007. A test case for anomalous fading correction in IRSL dating. *Quaternary Geochronology* **2**: 216–221. DOI:10.1016/j.2006.05.014.
- Westaway R, Pringle M, Yurtmen S, Demir T, Bridgland D, Rowbotham G, Maddy 7D. 2004. Pliocene and Quaternary regional uplift in western Turkey: the Gediz River terrace staircase and the volcanism at Kula. *Tectonophysics* **391**: 121–169.
- Westaway R, Guillou H, Yurtmen S, Beck A, Bridgland D, Demir T, Scaillet S, Rowbotham G. 2006. Late Cenozoic uplift of western Turkey: improved dating of the Kula Quaternary volcanic field and numerical modelling of the Gediz River terrace staircase. *Global and Planetary Change* **51**: 131–171.
- Wijbrans J, Schneider B, Kuiper K, Calvari S, Branca S, De Beni E, Norini G, Corsaro RA, Miraglia L. 2011. <sup>40</sup>Ar/<sup>39</sup>Ar geochronology of Holocene basalts; examples from Stromboli, Italy. *Quaternary Geochronology* **6**: 223–232.

## Supporting Information

Additional supporting information may be found in the online version of this article at the publisher's web site.